

Improvement of Mechanical Properties and Work-Hardening Behavior of Intercritically Annealed Dual Phase Steel

M. Zamani¹, H. Mirzadeh^{*2}, M. Maleki³, F. Jamei⁴

School of Metallurgy and Materials Engineering, College of Engineering, University of Tehran, P.O. Box 11155-4563, Tehran, Iran

Abstract

The effect of the initial microstructure and intercritical annealing on mechanical properties and work-hardening response of a high-formability low carbon steel were studied. The work-hardening analysis was based on the modified Crussard–Jaoul method. The ferritic-pearlitic sheets showed low strength and high total elongation with the appearance of the yield point phenomenon. The occurrence of yield-point phenomenon resulted in the very low work-hardening rates at the initial stages of deformation. However, after intercritical annealing, a good combination of tensile strength and ductility along with much better work hardening response was observed. Intercritical annealing of martensite initial microstructure was found to be a viable technique for graining refinement of DP steels with much better tensile strength compared with that obtained by intercritical annealing of the normalized microstructure. These observations were related to the much finer microstructure and enhancement of work-hardening behavior in the former, where its work-hardening rate at each given true stress was considerably higher.

Keywords: Dual phase steels; Initial microstructure; Mechanical properties; Strain hardening rate.

1. Introduction

Advanced High Strength Steels (AHSS) with high strength, improved formability and crash worthiness compared with the conventional steel grades have been considered as viable materials for automotive applications. As one of the main categories of AHSS, the dual

phase (DP) steels normally have a duplex ferritic-martensitic microstructure. The chemical composition of these low carbon steels is simple (which is advantageous for weldability), they have high tensile strength with maintaining good ductility, and show high work hardening rates¹⁻⁴.

At a given martensite fraction, the mechanical properties and work-hardening behavior of the DP steels are largely determined by the morphology, size, and distribution of the martensite and also ferrite grain size. In this respect, Mirzadeh et al.⁴, Kalhor and Mirzadeh⁵, Cai et al.⁶, Das et al.⁷, Ahmad et al.⁸, Schemmann et al.⁹, and Seyedrezai et al.¹⁰ showed that changing the initial microstructure can significantly affect the attributes of the DP microstructure and the resulting mechanical properties. The martensite initial microstructure was experimentally found to be one of the appropriate ones for obtaining a good combination of mechanical properties⁴⁻⁸. This needs to be evaluated for other DP steels, especially for those with low amount of C and Mn that inhibits the

** Corresponding author*

Tel: +98 21 82084080; Fax: +98 21 88006076

E-mail: hmirzadeh@ut.ac.ir

Address: School of Metallurgy and Materials Engineering,

College of Engineering, University of Tehran, P.O. Box

11155-4563, Tehran, Iran

1. M.Sc. Student

2. Associate Professor

3. B.Sc.

4. B.Sc.

formation of completely martensitic microstructure upon quenching from the austenitization temperature.

The largest category of low-carbon steels is flat-rolled products (sheet or strip), usually in the cold-rolled and annealed condition. The carbon content for these high-formability steels is very low, less than 0.10 wt. % C, with up to 0.4 wt. % Mn. Typical uses are in automobile body panels, tin plate, and wire products. By consideration of the low amount of C and Mn, achieving fully martensitic microstructure will be unlikely^{11, 12)} and these steels might exhibit a DP microstructure when they are quenched from the austenitization temperature. Obtaining DP microstructures from these kinds of steels and investigating their mechanical properties might broaden their potential industrial applications. Accordingly, the present work has been dedicated to study the effect of the initial microstructure and intercritical annealing on mechanical properties and work-hardening response of a high-formability steel with low C and Mn content.

2. Experimental Details

A low carbon steel sheet with chemical composition (wt. %) of 0.035C-0.268Mn-0.035Si which was in fully annealed condition was used in this work, The A₁ and A₃ temperatures were respectively estimated as 736 °C and 890 °C by Trzaska equations (Eq. 1)¹²⁻¹⁴⁾. The schematic representation of the processing routes used in this work is shown in Fig. 1a. The As-Received steel was heated to 1050 °C and held at this temperature for 15 min and then (I) air cooled to obtain a fine and uniform ferritic-pearlitic microstructure (Normalized steel) and (II) water quenched to obtain a dominantly martensitic microstructure (Quenched steel). The Normalized and Quenched steels were considered as the initial sheets for intercritical annealing at 800 °C for 5 min to produce DP_N and DP_Q steels respectively. The choice of intercritical annealing time was based on the preliminary experiments with the aim of obtaining the equilibrium fractions of the phases.

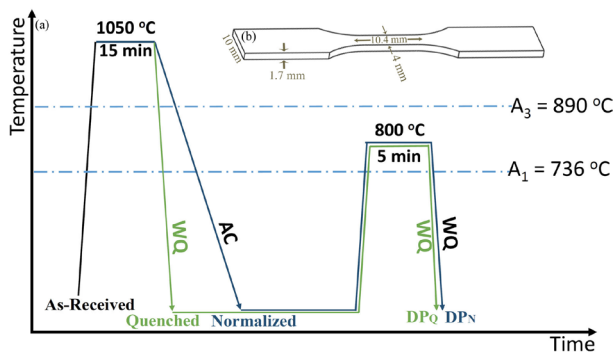


Fig. 1. Schematic representation of the (a) processing routes employed in this study and (b) tensile test specimen. AC and WQ represent air cooling and water quenching, respectively.

$$A_1 = 739 - 22.8C - 6.8Mn + 18.2Si + 11.7Cr - 15Ni - 6.4Mo - 5V - 28Cu$$

$$A_3 = 937.3 - 224.5\sqrt{C} - 17Mn + 34Si - 14Ni + 21.6Mo + 41.8V - 20Cu$$

Eq. (1)

The microstructural observations were performed after etching by the LePera's reagent (1 g Na₂S₂O₅ in 100 ml H₂O + 4 g picric acid in 100 ml ethanol) followed by Nital solution. Tensile test specimens were prepared according to JIS Z 2201 standard with gauge length of 10.4 mm (Fig. 1b). Tensile testing was carried out at room temperature by a computerized testing machine (SANTAM STM-20) at the constant cross-head speed of 1 mm/min. Vickers hardness measurements were based on the load of 30 kg.

The modified Crussard-Jaoul analysis¹⁵⁻¹⁸⁾ was also used, which was based on $\varepsilon = A + B\sigma^p$, where A , B , and p are constants. Therefore $\sigma = \sqrt[p]{(\varepsilon - A)/B}$, then, $d\sigma/d\varepsilon = \sigma/(p(\varepsilon - A))$, and finally $\ln(d\sigma/d\varepsilon) = (1 - p)\ln\sigma - \ln(pB)$. As a result, double-logarithmic plots can be used to analyze work-hardening behavior. It should be noted that the values of the work-hardening rate ($d\sigma/d\varepsilon$) were calculated based on the central difference approach¹⁹⁻²¹⁾ expressed as $d\sigma/d\varepsilon|_i = \{\sigma_{i+1} - \sigma_{i-1}\} / \{\varepsilon_{i+1} - \varepsilon_{i-1}\}$.

3. Results and Discussion

3.1. Before intercritical annealing

Fig. 2a shows that the As-Received microstructure exhibits a ferritic-pearlitic banded microstructure^{22, 23)}. The formation of banded structure in steels can be explained by the microsegregation of some alloying elements (particularly Mn) between dendrite arms

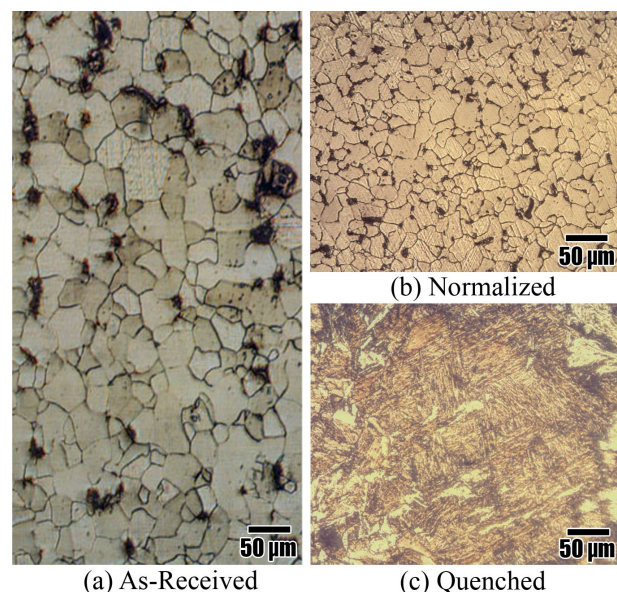


Fig. 2. Optical micrographs of (a) As-Received steel, (b) Normalized steel, and (c) Quenched steel.

during solidification and subsequent pancaking of Mn-lean and Mn-rich areas during rolling operations. During cooling to room temperature, the Mn-lean areas with higher A_3 temperature transform to ferrite, and in this way, alternative bands of ferrite and pearlite appear in the microstructure^{4, 24, 25}. The microstructure of Normalized steel is shown in Fig. 2b, which shows a finer ferritic-pearlitic microstructure (average ferrite grain size of $\sim 17 \mu\text{m}$) compared with the As-Received microstructure (average ferrite grain size of $\sim 36 \mu\text{m}$). The microstructure of the Quenched steel is also shown in Fig. 2c, which reveals the presence of martensite laths and some amount of ferrite ($\sim 10 \text{ vol}\%$). The presence of ferrite in the quenched microstructure is related to the low hardenability of this steel with very low C and Mn contents, and as a result, some amount of ferrite forms during transfer of the sheet from furnace to the quenching medium.

Tensile stress-strain curves of these samples are shown in Fig. 3a. It can be seen that the Normalized steel exhibited higher yield strength but lower ductility compared with the As-Received steel, which was related to the finer grain size of the Normalized steel. Moreover, both steels showed a well-defined yield point phenomenon, which is believed to be related to the Cottrell atmospheres produced by interstitial atoms around dislocations^{1, 4}. The Quenched steel, however, exhibited high strength and low ductility due to its martensitic nature. The similar trend can be seen in Fig. 3b for hardness values.

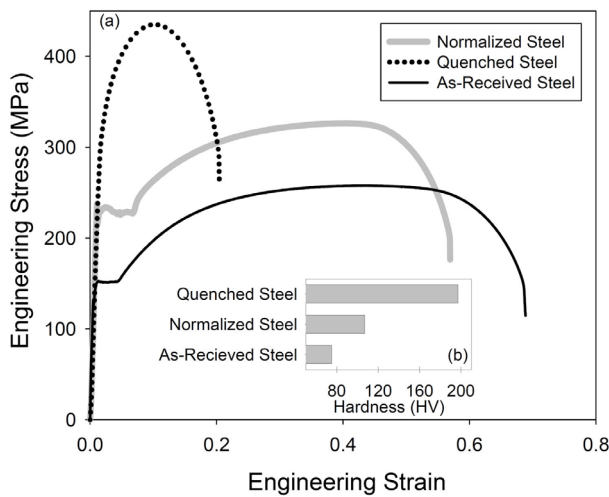


Fig. 3. Mechanical properties before intercritical annealing: (a) Tensile stress-strain curves, (b) Hardness values.

3. 2. After intercritical annealing

Based on the Normalized steel, some dual-phase microstructures were produced by holding the sheets for 15 min at temperatures between $750 \text{ }^\circ\text{C}$ to $1050 \text{ }^\circ\text{C}$ followed by quenching. Accordingly, the resultant microstructures and martensite fractions are also

shown in Fig. 4. It can be seen that by increasing the intercritical annealing temperature, the volume fraction of martensite increases. However, this trend is also valid for annealing temperatures above A_3 , which is related to the low hardenability of this steel as discussed above. The intercritical annealing at $800 \text{ }^\circ\text{C}$ with $\sim 28 \text{ vol}\%$ martensite was chosen to investigate the effect of initial microstructure.

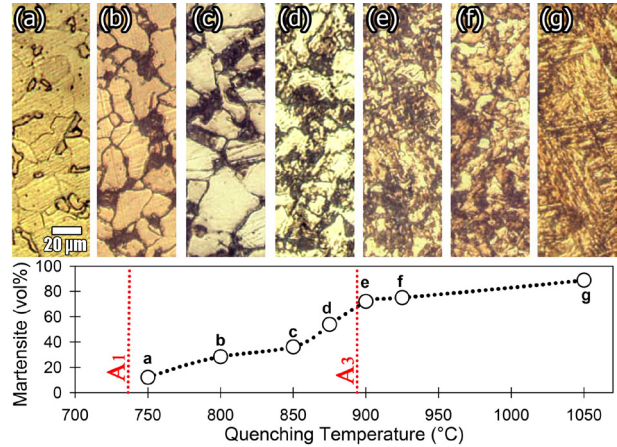


Fig. 4. Microstructure and martensite volume fraction after quenching from different temperatures.

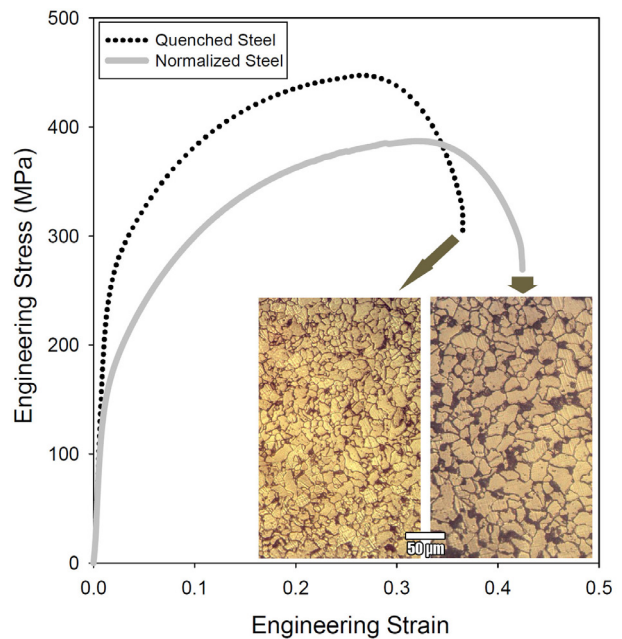


Fig. 5. Microstructure and mechanical properties after intercritical annealing of Normalized and Quenched steels.

Fig. 5 shows the microstructure and mechanical properties after intercritical annealing of Normalized and Quenched steels. Both DP steels exhibit continuous yielding behavior, which can be related to the austenite to martensite transformation (during quenching from

Table 1. Average ferrite grain size and average size of martensite islands.

Property	Average ferrite grain size (μm)	Average size of martensite islands (μm)
DP_N	15.2	8.8
DP_Q	8.1	4.5

the intercritical region). The shear and volume changes associated with the transformation generate some unpinned dislocations in ferrite, which can inhibit the occurrence of yield-point phenomenon^{4,11}). It can be also seen in Fig. 5 that the DP microstructure produced from the initial Quenched microstructure (DP_Q) is much finer than DP_N (Table 1). This can be ascribed to the fine initial microstructure comprising of laths, blacks, pockets, and prior austenite grain boundaries, which provides abundant nucleation sites during intercritical annealing. The finer ferrite grain size is responsible for the increased yield strength of ~ 60 MPa.

The work-hardening rate plots based on the modified Crussard–Jaoul analysis is shown in Fig. 6. It can be seen that the Normalized steel shows low work-hardening rates at the initial stages of deformation due to the occurrence of yield-point phenomenon. For the DP_N steel, the work-hardening rate at each given true stress is considerably higher. Moreover, three stages of work-hardening can be detected for the DP_N steel: The transient Stage I represents the glide of mobile dislocations in ferritic areas near the martensitic regions, Stage II belongs to the deformation of the constrained ferrite, and Stage III is related to the concurrent deformation of martensite and hardened ferrite¹⁵⁻¹⁸). Moreover, the work-hardening curve corresponding to DP_Q steel is located above that of DP_N steel, which reveals that the work-hardening behavior of DP_Q steel is better. It has been also shown

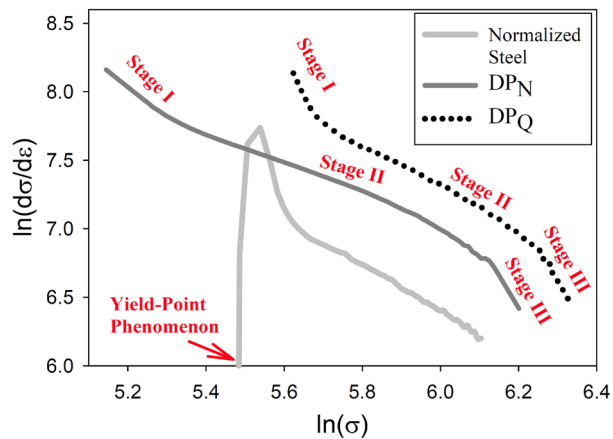


Fig. 6. Work-hardening rate plots based on the modified Crussard–Jaoul analysis.

that the work-hardening rate ($d\sigma/d\varepsilon$) of DP steels can be related to $\sqrt{V_M/D_M}$ ^{1,4,26}), where V_M and D_M are respectively the martensite volume fraction and average size of martensite islands. At a given V_M , by decreasing D_M , the work-hardening capability enhances, which is consistent with the abovementioned discussion.

4. Conclusions

The effects of the initial microstructure and intercritical annealing on mechanical properties and work-hardening response of a high-formability steel with low C and Mn content were studied. The following conclusions can be drawn from this work:

- The as-received steel exhibited low strength and high total elongation with the appearance of the yield point phenomenon. After normalizing heat treatment, a finer microstructure was obtained with the average ferrite grain size of ~ 17 μm compared with that of the as-received steel (~ 36 μm). This grain refinement resulted in ~ 80 MPa and 70 MPa enhancements in yield stress and tensile strength respectively.
- The DP microstructure obtained by intercritical annealing of the normalized steel showed a good combination of tensile strength and ductility along with much better work hardening response. As a result of the initial coarse microstructure, in the DP microstructure, the ferrite grain size was large (~ 15.2 μm) and the martensite islands (~ 8.8 μm) were relatively coarse. However, the DP microstructure produced from the initial Quenched microstructure was much finer (ferrite grain size of ~ 8.1 μm and martensite islands of ~ 4.5 μm), which was ascribed to the fine initial martensitic microstructure.
- Intercritical annealing of martensite initial microstructure was found to be a viable technique for grain refinement of DP steels with much better tensile strength compared with that obtained by intercritical annealing of the normalized microstructure. These observations were related to the much finer microstructure and enhancement of work-hardening behavior in the former.

References

- [1] Y. Mazaheri, A. Kermanpur, A. Najafzadeh: ISIJ Int., 55(2015), 218.
- [2] H. Ashrafi, M. Shamanian, R. Emadi, N. Saedi:

- Mater. Sci. Eng. A., 680(2017), 197.
- [3] H. Mirzadeh, M. Alibeyki, M. Najafi: Metall. Mater. Trans. A., 48(2017), 4565.
- [4] X. L. Cai, A. J. Garratt-Reed, W. S. Owen: Metall. Trans. A., 16(1985), 543.
- [5] D. Das, P. P. Chattopadhyay: J. Mater. Sci., 44(2009), 2957.
- [6] E. Ahmad, T. Manzoor, M. M. A. Ziai, N. Hussain: 21(2012), 382.
- [7] L. Schemmann, S. Zaefferer, D. Raabe, F. Friedel, D. Mattissen: Acta Mater., 95(2015), 386.
- [8] H. Seyedrezai, A. K. Pilkey, J. D. Boyd: Mater. Sci. Eng. A., 594(2014), 178.
- [9] G. Krauss: Steels Processing, Structure and Performance, 2nd edition, ASM International, 2015.
- [10] M. Maleki, H. Mirzadeh, M. Zamani, Steel Res. Int., 89(2018), 1700412.
- [11] A. A. Gorni: Steel Forming and Heat Treating Handbook, www.gorni.eng.br, 2012.
- [12] A. Bag, K. K. Ray, E. S. Dwarakadasa: Metall. Mater. Trans. A., 30(1999), 1193.
- [13] T. S. Byun, I. S. Kim: J. Mater. Sci., 28(1993), 2923.
- [14] B. Krebs, L. Germain, A. Hazotte, M. Goune: J. Mater. Sci., 46(2011), 7026.
- [15] S. W. Thompson, P.R. Howell: Mater. Sci. Techn., 8(1992), 77.
- [16] N. K. Balliger and T. Gladman: Met. Sci., 15(1981), 95.
- [17] T.S. Byun, I.S. Kim: J. Mater. Sci., 28(1993), 2923.
- [18] S. Ghaemifar, H. Mirzadeh: Can. Metall. Q., 56(2017), 459.
- [19] M. Najafi, H. Mirzadeh, M. Alibeyki: IJMF., 5(2018), 19.
- [20] S. Saadatkia, H. Mirzadeh: J. M. Cabrera, Mater. Sci. Eng. A., 636(2015), 196.
- [21] H. Mirzadeh, J. M. Cabrera, J. M. Prado, A. Najafzadeh: Mater. Sci. Eng. A., 528(2011), 3876.
- [22] B. Krebs, L. Germain, A. Hazotte, M. Goune: J. Mater. Sci., 46(2011), 7026.
- [23] S. Deldar, H. Mirzadeh, M.H. Parsa: Eng. Fail. Anal., 68(2016), 132.
- [24] S. W. Thompson, P. R. Howell: Mater. Sci. Techn., 8(1992), 77.
- [25] G. Azizi, H. Mirzadeh, M.H. Parsa: Mater. Sci. Eng. A., 639(2015), 402.
- [26] N. K. Balliger and T. Gladman: Met. Sci., 15(1981). 95.